Scanning Electron Microscopy

Volume 1982
Number 1 *1982*

Article 31

1982

Generation, Collection and Properties of an SE-I Enriched Signal Suitable for High Resolution SEM on Bulk Specimens

Klaus-Ruediger Peters
Yale University School of Medicine

Electron Beam Interactions With Solids (Pp. 363-372)
SEM, Inc., AMF O'Hare (Chicago), IL 60666, U.S.A.

GENERATION, COLLECTION AND PROPERTIES OF AN SE-I ENRICHED SIGNAL SUITABLE FOR HIGH RESOLUTION SEM ON BULK SPECIMENS

Klaus-Ruediger Peters

Section of Cell Biology, Yale University School of Medicine
333 Cedar Street, New Haven, CT 06510

ABSTRACT

At useful magnifications of 100,000 to 200,000 times, high topographic resolution becomes possible on bulk specimens with a secondary electron (SE) signal, generated by the probe at the site of incidence (SE-I signal), if SE, generated in the microscope chamber or the column by BSE or by electrons of the probe, are suppressed. BSE-dependent SE make up to 90% of the collected SE signal and add to the SE-I signal a high noise component that deteriorates topographic SE-I contrasts. SE-III, produced by BSE at the lower pole piece of the microscope, account for 60-70% of the SE signal. SE-III generation is eliminated by shielding the pole piece with an electron adsorption device. The SE-IV signal component, produced by the electrons of the probe at the final apertures is reduced to 2-3% of the SE signal by using a large final aperture. SE-II, generated by emerging BSE at the surface of the specimen at some distance from the probe, are collected together with SE-I. SE-(I + II) images obtained from bulk gold crystals under such improved conditions for signal collection show small particles of 4-5 nm in size and edge brightness effects 2-3 nm in width. The cores of ferritin molecules adsorbed on bulk carbon are imaged in appropriate size of $\sim$ 5.5 nm. At high magnifications, contrasts of small topographic features are expected to be produced mainly by SE-1.

Keywords: High resolution SEM on bulk specimens; field emission microscopy; SE-I signal; SE-III signal component; SE-IV signal component; Topographic contrasts.

Contact: Dr. Klaus-Ruediger Peters
Section of Cell Biology
Yale University School of Medicine
333 Cedar Street, New Haven, CT 06510
(203) 785-4306

INTRODUCTION

In scanning electron microscopy (SEM), high resolution signals are generated on bulk specimens by electrons of the probe (primary electrons – PE) at the specimen surface and are emitted from the spot of incidence (White et al., 1968; Everhart, 1968; Reimer et al., 1968). The signals consist of backscattered electrons (BSE), secondary electrons (SE), and Auger electrons (AE). Resolution depends on the probe diameter, the excitation surface area, and the signal-to-noise ratio (S/N-ratio) in the collected signal (Wells, 1974). High resolution signals are defined here as signals used for imaging small particles in material – or topographic contrasts with a microscope operated at useful magnifications. At such magnifications, structural details having the dimensions of the probes' diameter become visible in the image.

AE are emitted from the specimens in such low numbers that the AE signal is not suitable for high magnification imaging because of its low S/N-ratio (Wells, 1974). BSE and SE are generated in sufficient numbers if high brightness electron sources – LaB_6 or field emitter – are used. High resolution BSE (BSE-I), generated on bulk specimens with low energy loss in the area of incidence of the probe, differ from other BSE (BSE-II), which emerge after multiple scattering and high energy loss at some distance from the probe. BSE-I emission increases at high tilt angles of the specimen (increase of S/N-ratio) and under such conditions the BSE-I signal can be collected with high specificity and efficiency using an energy filter (Wells, 1971). With this BSE-I signal, collected from tilted, bulk-metal or gold decorated specimens (Wells et al., 1973; Broers et al., 1975), high resolution in SEM has been demonstrated in material and topographic contrasts (low-loss image mode). Unfortunately, the high resolution SE signal (SE-I), generated in the incident area of the probe, cannot be distinguished or separated from other SE (SE-II) which are generated by the BSE-II in the specimen. However, it has been calculated (Wells, 1974; 1975) and demonstrated (cit. Wells, 1974) that the SE signal (SE-I + II) can give in material contrast as good a resolution as the BSE-I signal, when generated on and collected from tilted specimens. In topographic contrast, however, the resolution obtained with the SE signal (SE-I + II) is found to be much lower than that given by the BSE-I signal. In the case of untilted specimens and at high magnifications, the SE-I signal is

expected to be superior to the BSE-I signal for both material and topographic contrasts (George and Robinson, 1976; 1980).

The predicted high resolution SE-I contrasts could not be verified on bulk untilted specimen with any microscope (George and Robinson, 1977a) until the collection for the SE-I signal was improved (Peters et al., 1981). It could be shown that the high magnification information is associated only with SE-I and not with SE-II or BSE (Peters, 1982). In this paper, the new procedures for the generation and collection of the SE-I signal are described and the imaging properties of the signal are characterized.

MATERIALS AND METHODS

Microscope and Detectors. A cold field emission SEM (JEOL JFSM 30, JEOL U.S.A. Inc., Peabody, MA 01960) was used at 30 keV acceleration voltage with a measured beam current of $2 - 4 \times 10^{-11}$A. The specimens were placed untilted at 13 mm working distance. The diameter of the beam was inferred from the smallest dimensions ($\sim$1.0 nm width) of filamentous structures resolved on biological specimens coated with Cr. Beneath the pole piece of the lower lens, a BSE-to-SE converter (Volbert and Reimer, 1980) was installed and used in conjunction with an Everhart-Thornley detector. All high magnification micrographs were taken at a CRT magnification of 200,000 times in 50 sec. SEM images were recorded on Polaroid Film Type 55.

High resolution test specimens. A gold crystal specimen prepared by gold evaporation onto heated carbon, was obtained from the JEOL Inc. USA. Carbon supports (polished pyrolytic planchets) were covered with thin formvar films and coated with a 10.0 nm thick layer of carbon. Ferritin, obtained from Sigma, St. Louis, MO 63178 (No. F-4303), was adsorbed onto supports (prepared as above) and critical point dried from CO_2.

RESULTS

In the conventional SE imaging mode (SEI) the Everhart-Thornley detector (E-T detector) collects not only specimen-specific SE but also SE generated in the microscope. The contribution of these signal components to the high resolution image was experimentally examined for different specimens in a microscope with a large working distance.

I. Signal collection.

The components of the SE signal collected by an E-T detector are (Fig. 1): the high resolution signal (SE-I) produced by the primary electrons (PE); the SE-II excited by the BSE-II; the SE-III generated by BSE at the pole piece of the lower lens and at other parts of the specimen chamber; and the SE-IV coming from the final aperture. Generation of SE-III at the pole piece and their collection were controlled with a BSE-to-SE converter (Fig. 2). This converter was previously described for BSE detection (Volbert and Reimer, 1980). The converter consists of a copper plate, coated with MgO, electrically isolated and shielded against the E-T detector with a grounded grid. A negative potential applied to the converter plate releases the SE (SE-III) produced by BSE in the plate.

LIST OF SYMBOLS

B	=	Background signal collected with the BSE-to-SE converter
BSE	=	Backscattered electrons
δ	=	SE emission coefficient
η	=	BSE emission coefficient
SE	=	Secondary electron
σ	=	Total yield of SE
SEI	=	Secondary electron image
BSI	=	Backscattered electron image
E-T	=	Everhart-Thornley
PE	=	Primary electrons
PM	=	Photo multiplier
SE-I,II,...	=	SE-one, two, ...
SEM	=	Scanning electron microscope

A positive potential retains the SE so that the converter can be used as a BSE absorption plate as recently described (Peters et al., 1981; Peters, 1982). Depending on the applied converter bias two different signals are collected by the E-T detector. The SE signal is collected with a positive biased converter as SE-(I + II). The BSE signal is actually detected as SE-III and is collected with a negative biased converter together with the SE signal as SE-(I + II + III). Signal strength collected in both modes from different materials are proportional to the appropriate electron emission coefficients, i.e., the SE-(I + II) signal is proportional to δ and the SE-(I + II + III) signal is proportional to $\sigma = \delta + \eta$. Electron emission coefficients (Fig. 3) were determined in recent years by several investigators (Seiler, 1967; Reimer et al., 1968; Reimer, 1979). In all cases, an additional background signal which consists of SE-IV and some BSE is also collected by the E-T detector. The signal collection efficiency of the detector system was tested by examining material contrasts in images of appropriate specimens. The transfer function of the signal between the main signal amplifier and the printed micrograph was documented by the reproduction of gray wedge steps (Fig. 4), which represented linearly increasing signal voltages between O V (0% signal = black) and 6 V (100% signal = white). A test specimen, composed of C, Cr, Nb, and Au, was imaged under identical signal processing in two immediately following scans: the first with a negatively biased converter (Fig. 5a), and the second with a positively biased converters (Fig. 5b). A comparison of material contrasts given by the different metals (circles in both Figures) show good agreement with differences in the corresponding emission coefficients of the same materials (Fig. 3): i.e., $\sigma_C < \delta_{Au} < \sigma_{Cr}$.

II. The SE-IV signal component.

The SE-IV component and the relative ratio of collected SE and BSE were analyzed at the rim of a clean Pt aperture of a Faraday cage (Fig. 6a). The signal strengths were measured against a base line (line scan d) obtained from a line scan during which the SE detection was prevented by a negative bias applied to the E-T detector. SE-(I + II + III + IV) were collected with positively biased converter (line scan a) and SE-III were removed from the signal when the detector was negatively biased (line scan b). Over the Faraday cage opening only SE-IV were collected (line scan c) since all PE

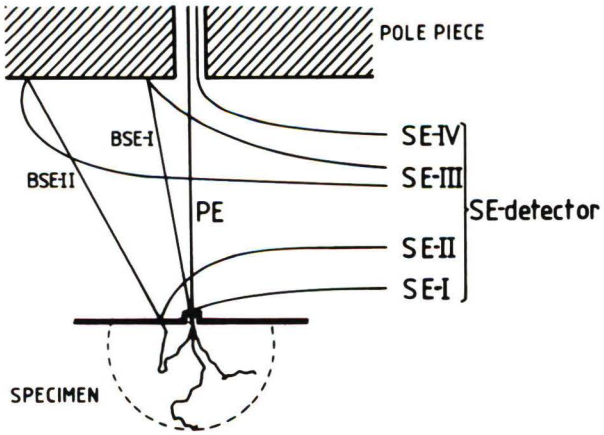

Fig. 1. Origin of the different components of the SE signal generated on a bulk specimen. PE = Primary electrons; SE = Secondary electrons; BSE = Backscattered electrons.

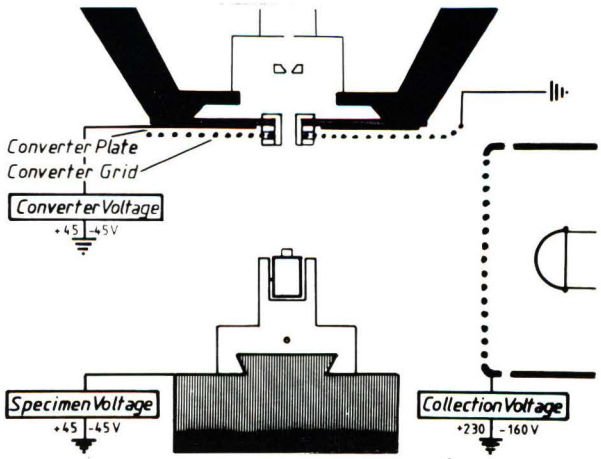

Fig. 2. BSE-to-SE converter. SE-III generated by BSE at the converter plate can be released by a negative bias or adsorbed by a positive bias applied to the latter.

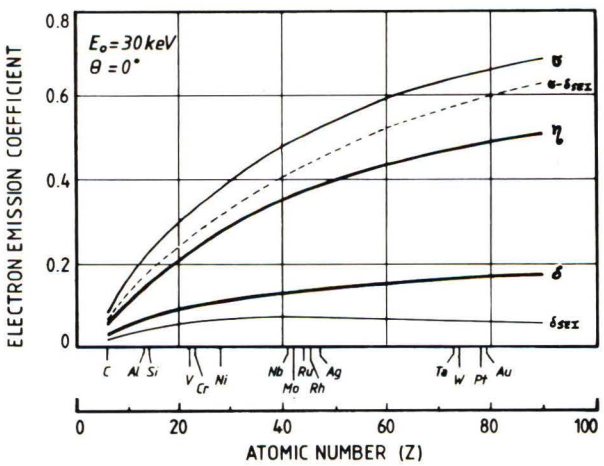

Fig. 3. Diagram of established electron emission coefficients: δ for SE and η for BSE. $\sigma = \delta + \eta$.

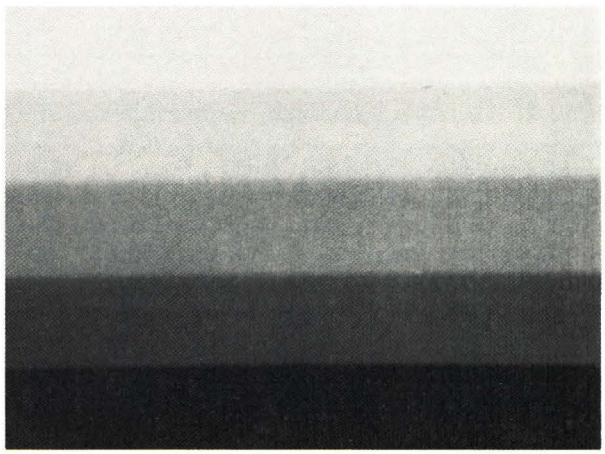

Fig. 4. Transfer function of the signal between main amplifier and printed micrograph. Signal steps are linear increasing from O V (black) to +6 V (white).

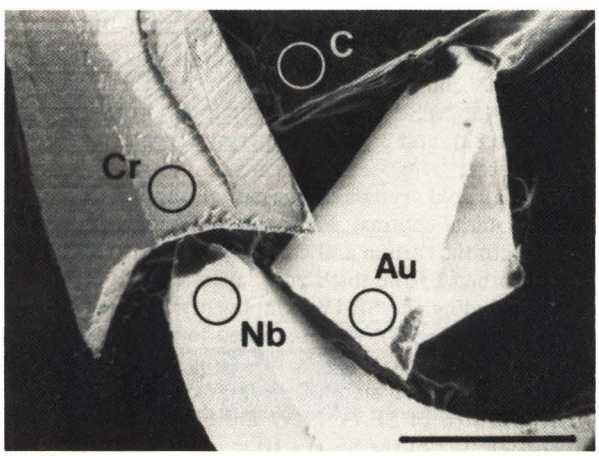

Fig. 5a. Image generated by an SE-(I + II + III + IV) signal; specimen composed of carbon (C), chromium (Cr), niobium (Nb), and gold (Au). Bar = 1 mm

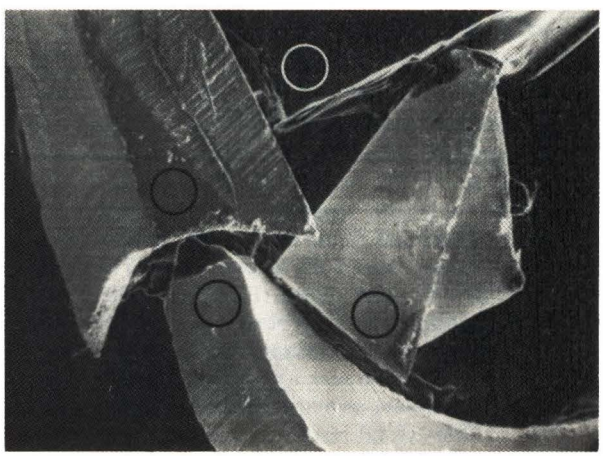

Fig. 5b. Image generated by an SE-(I + II + IV) signal of the same specimen as seen in Fig. 5a with unchanged signal processing. Circles show horizontal areas.

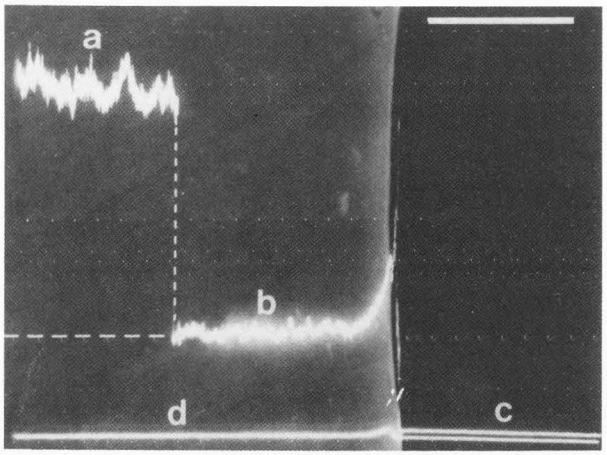

Fig. 6a. Image of the rim of the Pt aperture of a Faraday cage. Line scan of different signal modes. a = SE-(I + II + III + IV); b = SE-(I + II + IV); c = SE-IV; d = SE detection off. Bar = 2.5 μm.

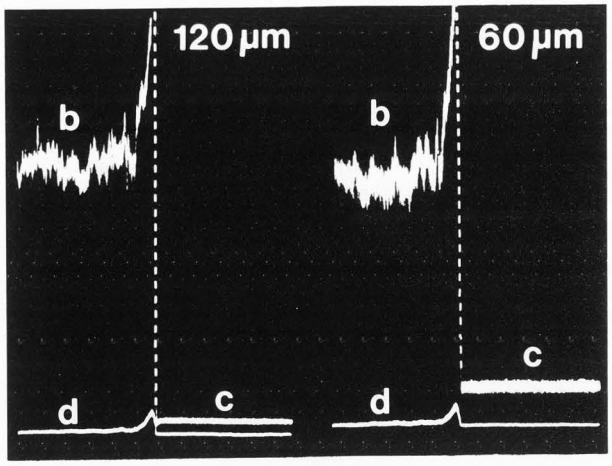

Fig. 6b. Line scan profiles through the same specimen as in Fig. 6a using in the SEM a 120 μm (left) and a 60 μm (right) objective lens aperture. b, c, d: as in Fig. 6a.

were trapped inside the cage. The line scan d dropped at the edge of the aperture to a lower level revealing a background signal originating from BSE which reached the E-T detector. The background value was measured as the difference of the signals collected over the Pt and over the opening. The background contributed to the total signal 2.5% of the SE-(I + II) component and was expected to change proportionately with BSE emission. The relative signal value for the SE-III was calculated as signal difference (a − b) and the relative SE-(I + II) signal value was obtained by subtracting the SE-IV signal from (b − d). BSE were collected as SE-III with an 82% collection efficiency relative to the SE-(I + II) collection (100%). The contribution of the SE-VI component to the SE signal was found to depend on the size of the final aperture (Fig. 6b). Its value was 6% of the SE-(I + II) signal for a 120 μm aperture and increased to 16% for a 60 μm aperture. All following micrographs were taken with a 120 μm aperture.

III. Test specimens for SE-I contrast imaging.

Two test specimens were used to describe the properties of the signals at high magnification: a gold crystal specimen for characterizing the image quality in material and topographic contrasts and a ferritin-on-carbon specimen for detecting of a "topographic noise".

Gold crystal test specimen. The gold crystal specimen consisted of monocrystals grown on a solid carbon substrate. It contained large crystals, measuring 150 to 200 nm in size and 50 to 100 nm in height, separated by ∿ 50 to 100 nm wide gaps, and small crystals found on the carbon substrate in the gaps and on the surface of the large crystals. The specimen was imaged in both signal modes (Figs. 7a, c). Since the SE-IV signal component could not be excluded in either mode it will only be mentioned if necessary. The entire SE-signal (SE-(I + II + III); Fig. 7d line scan a) imaged crystals of all sizes on the carbon support primarily in material contrast (Fig. 7a). The smallest crystal resolved measured 2.0 to 2.5 nm. The topographic contrast on the large crystal surfaces was poor; it consisted of low edge brightness and low relief contrast. The signal contribution of the SE-(I + II) to this image was revealed after elimination of the SE-III. The residual signal (Fig. 7d line scan b), which included the SE-IV component, was ∿ 1/3 of the total signal and was displayed on the cathode-ray tube (CRT) with unchanged amplifier gain by adding an appropriate DC level to the signal (Fig. 7b). Details imaged by this SE-(I + II) signal component matched nearly completely all fine structural details seen in the image of the entire signal (Fig. 7a); i.e., edge brightness of the large crystals and all images of small crystals below 20 nm in size. Signal differences between the two imaging modes (Figs. 7a, b) could be accounted for by the SE-III component as increased material contrast of crystals larger than 20 nm. None of the topographic contrast elements were recognized by the SE-III. Amplification of the SE-(I + II) signal (including the SE-IV component) with the photo multiplier (PM) to the signal level of the combined signal (Fig. 7d line scan c) revealed new topographic details on the large crystals (Fig. 7c arrowheads). Smallest crystals of 4.0 to 5.0 nm in size were recorded in particle contrast as disks of homogenous brightness. Particles larger than 10.0 nm were seen with bright rims of 1.0 to 2.0 nm in width (Fig. 7c arrows).

A first evaluation of the relative proportion of the SE-signal components was made from line scans through the specimen similar to Fig. 7d under the following assumptions: 1.) the SE-IV component equals 6% of the SE emission coefficient of Au; 2.) SE and BSE are collected with similar efficiency (1:0.82); and 3.) the large crystals represent flat bulk gold surfaces.

The small gold crystals on the carbon support were visualized in material contrast. PE, penetrating through the small crystals into the carbon and emerging as BSE to the surface, were adsorbed by the thick gold layer. The SE-(I + II + III) signal (including the SE-IV component) collected from the small crystals (Fig. 8), was composed to 40% SE-III, which were generated by BSE originating from the small crystal itself or from adjacent sides of the large crystals. The residual signal consisted of SE-IV (3%) and SE-(I + II) (57%). Approximately 1/2 of the SE-(I + II) component was generated on the small crystals.

The small particles on the surface of the large crystals (Fig. 9) were imaged in topographic contrast. The SE-(I + II + III + IV) signal from the flat gold surface was composed to 61%

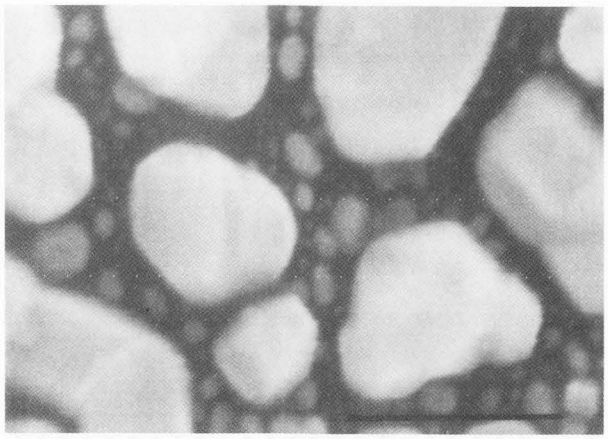

Fig. 7a. Gold crystal specimen imaged in SE-(I + II + III) mode. The image lacks topographic contrast and does not resolve details on the large crystals. Bar = 100 nm.

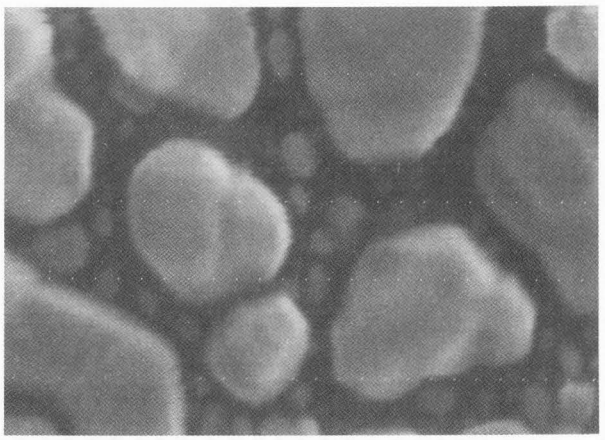

Fig. 7b. SE-(I + II) component of the entire SE signal (Fig. a). The image contains, in material and topographic contrast,all small details detected in Fig. 7a.

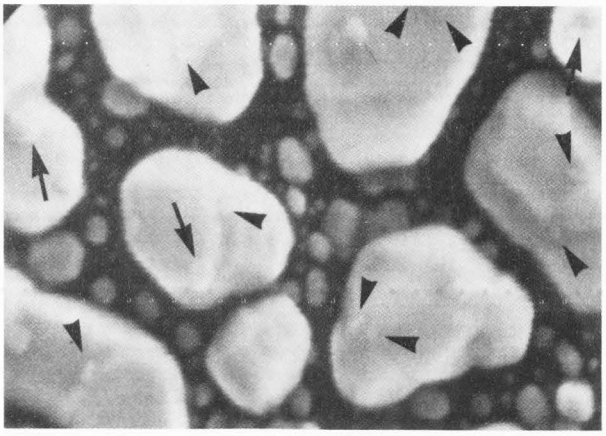

Fig. 7c. The same SE-I + II signal as in Fig. 7b, but PM amplified to the level of the complete SE signal. Good topographic contrast is detained and small crystals (arrowheads) become visible. Arrows show that particles larger than 10 nm have bright rims of 1 to 2 nm in width.

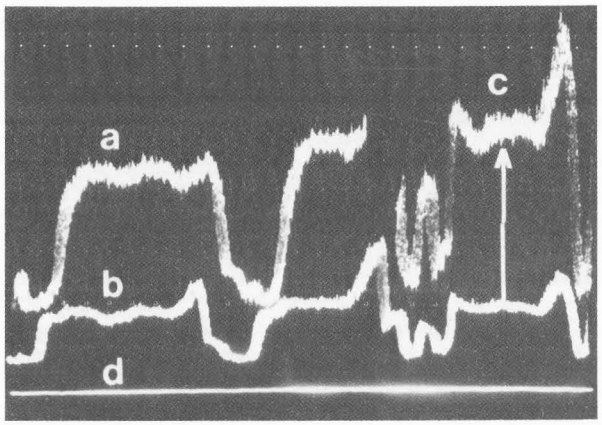

Fig. 7d. Line scan profiles through gold crystal specimen. a: SE-(I + II + III + IV) (Fig. 7a); b: SE-(I + II + IV) of a (Fig. 7b); c: SE-(I + II + IV) PM-amplified (Fig. 7c); d: SE,detection off.

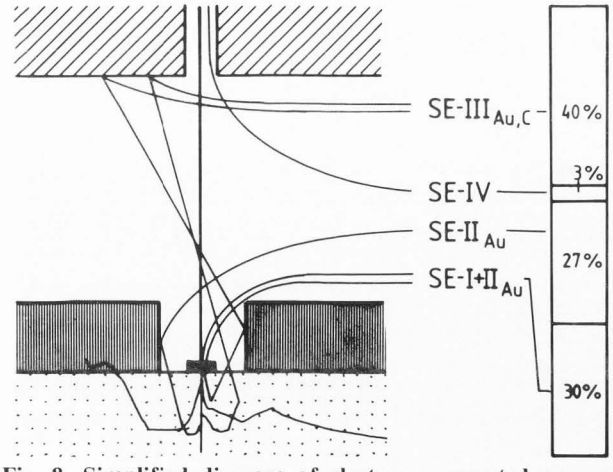

Fig. 8. Simplified diagram of electrons generated on, and signal collected from, small crystals grown among larger crystals.

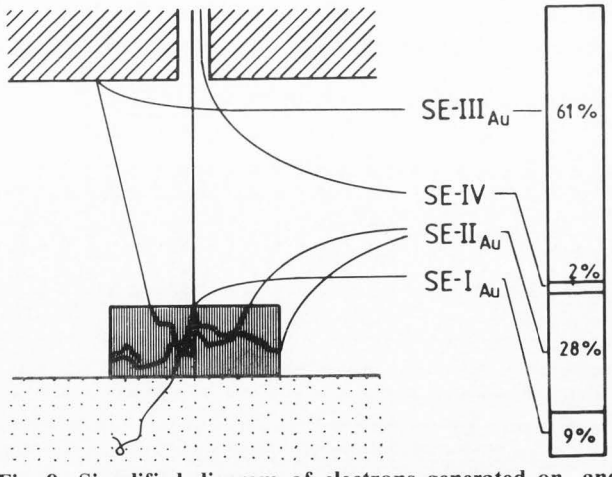

Fig. 9. Simplified diagram of electrons generated on, and signal collected from, the surface of large gold crystals.

of SE-III, generated by BSE at the converter beneath the pole piece. The remaining 39% of the signal consisted of SE-II (28%, which was generated by BSE in the specimen), SE-IV (2%) and SE-I (9%). The small particles could not be easily recognized with the entire SE signal; they were clearly visualized only after the elimination of 61% of the signal representing the SE-III component.

Ferritin-on-carbon specimen. A specimen with a topography of uniform small detail was provided by ferritin macromolecules deposited on smooth bulk carbon. Ferritin is 11 nm in diameter and is composed of a 5.5 nm large iron core enclosed by an apoprotein shell. In chains of ferritin molecules, cores and spacing between cores are of comparable dimensions. The cores were imaged with a signal composed of material and topographic components because they are elevated above the carbon support by their protein shells.

The SE-(I + II + III) signal produced an image of low contrast and considerable noise (Fig. 10a). The core spacings in ferritin chains were not clearly resolved (circle). Elimination of the SE-III signal component and PM-amplification of the residual signal to the level of the entire signal increased the S/N-ratio for the core images (Fig. 10b) and improved resolution of the core spacings (circle). In some areas of the specimen the protein shells of the ferritin were recognizable in topographic particle contrast. The line scan profile of the signals (Fig. 10c) revealed the origin of the strong noise component seen in the entire signal. The SE-(I + II + IV) signal component of the SE signal (line scan b) clearly displayed separated core signals which became irregularly distorted after addition of the SE-III signal component (line scan a). The SE-III signal apparently contained a high noise level.

A first evaluation of the relative proportions of the SE signal components generated at the iron cores (Fig. 11) was made assuming that: 1) the SE and BSE signals were collected with similar efficiency (1:0.82); 2) all BSE, generated in the carbon support, were collected; and 3) the ferritin particle, covering $\sim$ 1/2 of the surface, adsorbed 50% of the SE which were generated in the carbon support surface. BSE originating from the carbon support (1/5) and from the iron cores (4/5) produced $\sim$ 67% of the collected SE (SE-III). The remaining 33% of the signal was contributed by SE-IV (3%) and by SE-(I + II) (30%). One third of this latter component originated from the iron cores and the rest from the carbon support. The major signal component was produced by BSE from the iron cores. The signal was higher than expected and was probably caused by an increased collection efficiency of BSE due to multiple interactions with surrounding iron cores.

Contamination. On bulk, dense specimens, contamination deposition was a serious problem. Although all specimens were predegassed in high vacuum of 10^{-4} Pa ($\sim 10^{-6}$ Torr) and imaged at 10^{-6} Pa ($\sim 10^{-8}$ Torr) contamination build up was recognizable at high magnification after only a few scans. On bulk metals, thin contamination layers obscured topographic SE-I contrasts, and were seen as dark rings around the small particles of the gold crystal specimen (Fig. 12). Thicker layers obscured the SE signals completely as seen on an uncoated specimen of ferritin deposited onto bulk carbon (Fig. 13—upper right corner). However, on specimens of low density, i.e., biological tissues coated thin with low atomic number metals, contamination was never detected—even after prolonged observations—and it was not found to be a problem for high magnification imaging.

DISCUSSION

The observations reported in this paper confirm that high resolution images can be obtained with SE-I. Solid specimens and simplified experimental conditions were chosen to facilitate image interpretation and to improve understanding of conventional SE imaging contrasts. Specimens were placed untilted at a large working distance; operational parameters of the microscopes were measured; and test specimens with defined simple surface structures and composition were used.

Detector strategy. SE (SE-III) generated at the pole piece of the microscope have been determined as 10-50% (Everhart et al., 1959; Drescher et al., 1970; Moncrieff and Barker, 1978) of the total SE collected by an E-T detector. This BSE-to-SE conversion effect was used to increase collection efficiency of BSE (Moll et al., 1978; 1979). A further enhancement of BSE conversion was obtained by using a converter plate (Reimer and Volbert, 1979). It was assumed, however, that SE-III contribute a "fog" or background noise to the high magnification signal (Moll et al., 1978) and its elimination suggested (Reimer, 1979), although the extent to which they affect the high magnification image was not proven. A carbon coated BSE absorption plate, mounted beneath the pole piece, was shown to improve topographic resolution obtained on biological specimens (Peters et al., 1981), but no comparative experiments could be performed with such a plate. Therefore a BSE-to-SE converter was used here to analyze at high magnification the effects of adding or excluding the SE-III component of the signal.

BSE are converted by the BSE-to-SE converter into SE-III and are collected with the E-T detector with similar efficiency as SE-(I + II). The converter does not introduce significant noise to the SE-III signal (Baumann and Reimer, 1981). On this account this detector system allowed direct comparison of the imaging properties of the BSE signal and the SE signal. The amount of SE-III generated by the grounded converter was always lower than with the negative biased converter and similar to that obtained with the unprotected pole piece (Moll et al., 1979). When SE-III were retained by a positively biased converter, other BSE were still detected (Fig. 6). The background produced by the converter lowers the image quality in the SE-(I + II) mode at high magnification. The carbon coated BSE absorption plate may reduce the volume of this background.

SE signals always contained a SE-IV component. The reported values for SE-IV range from 2 to 40% of the conventional collected SE signal, which included the SE-III (Moncrieff and Barker, 1978; Moll et al., 1979). When a 120 μm final aperture was used in the microscope, the SE-IV component was 6% of the SE-(I + II) collected from Pt which amounts to 2-3% of the entire SE signal (SE-I + II + III). Smaller apertures which increase the SE-IV component (Moncrieff and Barker, 1978) were not used. No further attempt to reduce the SE-IV was made in these experiments.

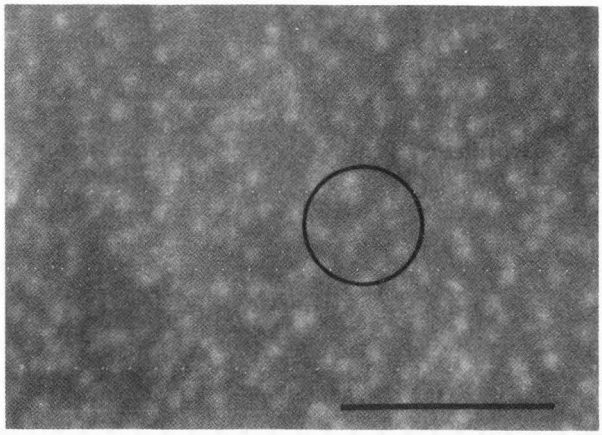

Fig. 10a. Ferritin-on-carbon specimen imaged in SE-(I + II + III) mode. With the entire signal, the spacings between ferritin cores (circle) are obscured. Bar = 100 nm.

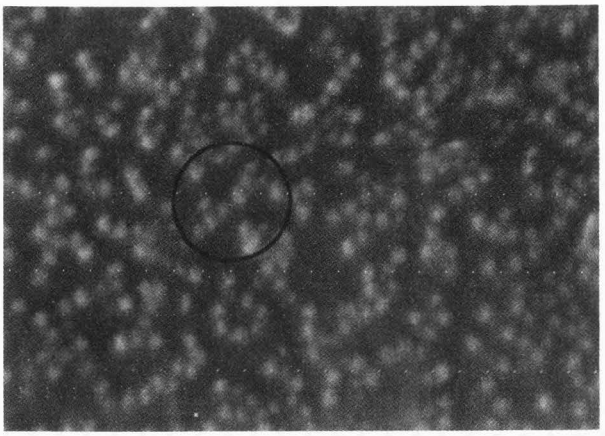

Fig. 10b. SE-(I + II) image of the same area as seen in Fig. 10a, PM-amplified. Core spacings are resolved (circle).

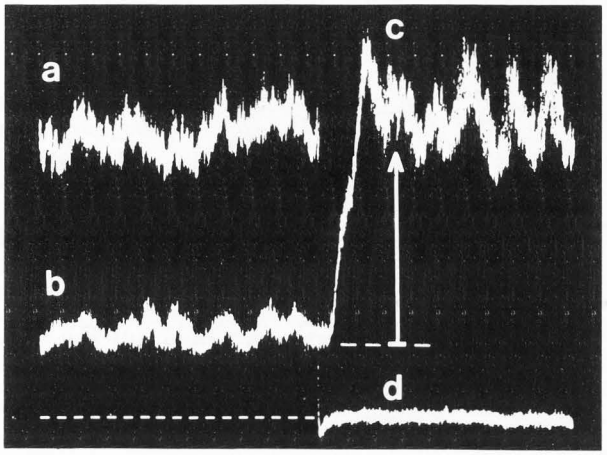

Fig. 10c. Line scan profile through ferritin-on-carbon specimen. a: SE-(I + II + III + IV) (Fig. 10a); b: SE-(I + II + IV); c: SE-(I + II + IV) PM-amplified (Fig. 10b); d: SE-detection off.

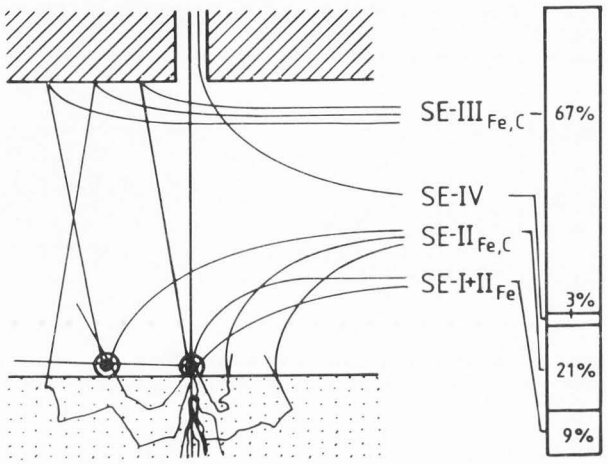

Fig. 11. Simplified diagram of electrons generated at the iron cores of the ferritin molecules and signal collected from the specimens.

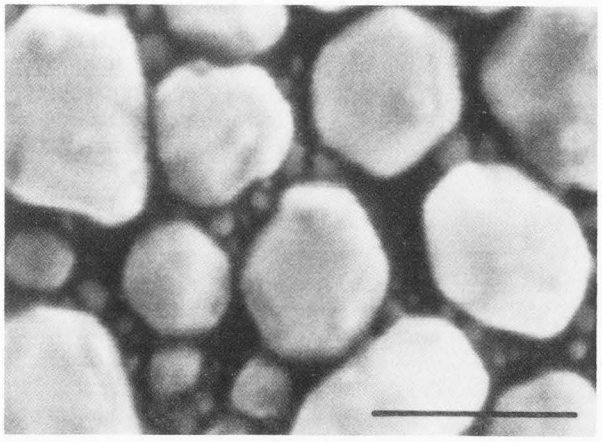

Fig. 12. Thin contamination layer on gold crystals seen in SE-I image mode. Note the dark and diffuse rings around small particles. Bar = 100 nm.

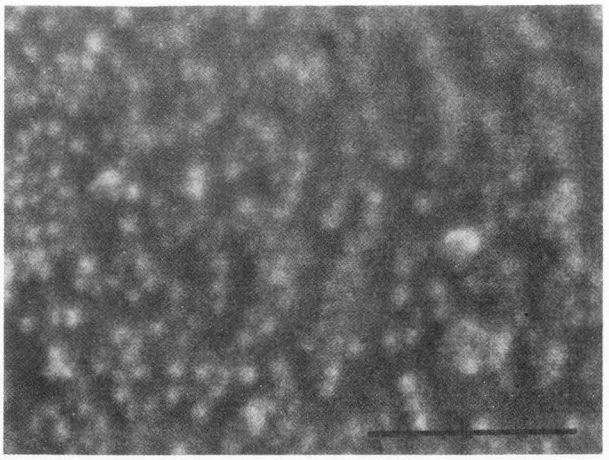

Fig. 13. Ferritin-on-carbon specimen, SE-I image mode. A heavy contamination layer obscures iron cores (upper right corner). Bar = 100 nm.

SE-I signal contrast generation. The possibility of generating contrast with the SE-I signal was already proved in "secondary electron imaging mode" (SEI) in high resolution micrographs of ferritin molecules under special conditions (Watabe et al., 1976). By using very thin carbon films as support, the SE-excitation volume of the signal was limited in width by the probe diameter and in depth to the summated thickness of the molecules and the support film. Under such conditions SE-II and SE-III generation is reduced and the individual particles may be imaged provided sufficient contrast be generated. In this case (Watabe et al., 1976), the molecules were decorated with Pt or Au crystals which increased electron scattering on individual molecules. The crystals accumulated specifically at topographic details which rose sharply from a flat support. On these accounts more SE were produced on the particles (and SE-III in the microscope), causing a "micro roughness contrast" (Peters, 1979) and producing an additional material contrast (thickness contrast). In fact, on such decorated specimens and in the conventional SEI-mode, the predominant SE contrasts are probably generated by BSE and are collected as SE-II + SE-III. Ultrathin continuous coatings of fine crystalline metals were used in previous studies to generate topographic contrast signals on bulk specimens on which (under untilted conditions) surface details smaller than 20 nm in size should be imaged exclusively by SE-I generated contrast, but not by BSE or BSE produced SE-II. However, high atomic number metals, like tantalum, did not improve the conventional SE images (SEI) of ferritin mounted on bulk carbon because a strong noise component deteriorated the topographic signal (Peters, 1979; 1980).

SE-I signal contrast detection. The SE-I contrast can be detected when the signal noise amplitude is smaller than that of contrast. Several well known noise components are included in the signal: gun shot noise, signal emission noise, detector noise, amplifier noise and recording noise (Everhart et al., 1959; Reimer, 1971; Swann and Smith, 1973; Wells, 1974; Baumann and Reimer, 1981). The highest noise component will limit the minimal detectable signal contrast (noise bottleneck). The ratio of signal to noise increases with increasing numbers of PE used to generate the signal; a certain minimum beam current is required to detect a certain contrast volume (Wells, 1974). Beam currents of $\sim 10^{-11}$A, applied within the beam diameter of $\sim$1.0 nm (1000 lines in 50 sec.), were found sufficient to generate detectable topographic SE-I contrast. Under such conditions, the noise bottleneck for the SE-I contrast was found in the BSE-dependent SE component of the signal.

On large gold crystals as well as on the ferritin specimen only $\sim$9% of the signal was SE-I, whereas 21-28% was contributed by SE-II and 61-67% by SE-III. The noise level was not increased when SE-III was eliminated and the SE(I + II + IV) signal was amplified (with a PM) to the level of the entire signal. This finding indicates that the gun shot noise component of the SE signal was not the cause for the deterioration of SE-1 contrasts. The noise components of detector and photomultiplier did also not account for the loss of SE-I contrast since the latter became visible after amplification of the SE-(I + II + IV) signal. Another origin of noise could be expected from the converter, where BSE generate SE-III. However, the converter has an exceptional low noise level (Baumann and Reimer, 1981). Since the emission noise was found greater for SE than for BSE (Reimer, 1971), the substantial contribution of SE-III ($\sim$67%) to the complete signal may have enhanced BSE-surface interactions causing a high frequency noise. Elimination of this noise component improved the detection of SE-I contrasts on the gold crystals. On the surface of the ferritin specimen, BSE were also scattered by the iron cores of ferritin molecules in the vicinity of the probe's impact point. The interaction of BSE with surface details of unequal distribution caused an additional low frequency signal variation which deteriorated the ferritin core images. This type of spatial signal alteration will be referred to as "topographic noise".

The influence of BSE on contrasts seen in the SE image and its relation to resolution were widely discussed in the recent past (George and Robinson, 1976; 1977a; 1977b; Wells, 1977; Reimer, 1979; Peters, 1979; Volbert and Reimer, 1980). Various views of contrast generation and signal collection were mostly restricted to medium or low magnification signals and led to the advocation of different specimen preparation procedures. Two different parameters are considered in this paper for visualizing specimen details smaller than 20 nm at high magnifications: material contrast signals and topographic contrast signals, both particle-specific.

For material contrast, SE-(I + II + IV) contained all information needed to visualize the small crystals grown on the carbon support. The smallest crystals recognized by BSE were 20 nm in size and were located close to large crystals (Fig. 8). At such locations collection efficiency of the BSE was increased due to additional scattering of the BSE at the larger crystals: a high SE-II component was added to the SE-I signal. Otherwise the BSE contained no information about smaller crystals and did not interfere with the recognition of the SE-I signal since they were collected only in low numbers (SE-I/SE-III = 1/1).

In case of topographic contrast, SE-III dominated the complete signal (SE-I/SE-III = 1/6) and increased resolution could be obtained with the SE-I signal only when SE-III collection was suppressed. This improved the contrast of the remaining SE-(I + II + IV) signal for all types of specimens.

The SE-II component of the signal was expected to be collected with the same efficiency as the SE-I component. The SE-I/SE-II ratio depends on specimen properties, i.e., its atomic number composition and its topography. It may be varied for certain specimens, of low atomic number composition or low density, by specimen preparation procedures and operational parameters of the microscope; i.e., on metal coated biological specimens or silicon substrates by the choice of metal type and acceleration voltage.

SE-I signal properties. High resolution surface information in topographic and material contrasts was found only in the SE-I signal component. SE-I are defined as SE generated by PE during the first scattering event in the specimen in a depth smaller than the escape depth of SE (SE-I escape from the site of generation within a distance equal to their range). SE-I and SE-II generated in the vicinity of the probe impact are not distinguishable and therefore, SE-II may contribute to some extent to the high resolution signal. For low incidence angles and low atomic-number metals an increase of SE-II and SE-I emission was calculated by Reimer and others (Reimer et al., 1968; Drescher et al., 1970; Reimer, 1979). Such an amplification phenomenon could generate very high

topographic contrasts seen as relief contrast and edge brightness. Not only at high magnifications, but also at low magnifications, the SE-(I + II + IV) signal generates brilliant images of high contrast.

CONCLUSIONS

The concept of high resolution SE-I imaging of bulk specimen uses several approaches to reduce the generation and the collection of BSE and BSE-originated SE. First the signal collection is improved by shielding the lower pole piece of the microscope with an electron absorption device. Secondly, the microscope is operated at high accelerating voltages to minimize the beam diameter, and to achieve sufficient beam current. At CRT magnifications of 100,000 to 200,000 times these procedures allow resolution with appropriate contrasts at the level of the beam diameter.

ACKNOWLEDGMENTS

The author gratefully acknowledges the support obtained by JEOL, Inc. U.S.A. in the form of gold crystal test specimens. The author thanks Ms. Cindy Davis for her excellent help in preparing and typing the manuscript. This work has been supported by NIH Grant Number 21714.

REFERENCES

Baumann W and Reimer L. (1981). Comparison of the noise of different electron detection systems using a scintillator-photomultiplier combination. Scanning **4**: 141-151.

Broers AN, Panessa BJ and Gennaro JF. (1975). High resolution SEM of biological specimens, Scanning Electron Microsc. 1975, 233-242.

Drescher H, Reimer L, and Seidel H. (1970). Backscattering and secondary electron emission of 10-100 keV electrons and correlation to scanning electron microscopy. Z.angew.Phys. **29**:331-336.

Everhart TE. (1968). Reflection on scanning electron microscopy, Scanning Electron Microsc. 1968, 3-12.

Everhart TE, Wells OC, and Oatley CW. (1959). Factors affecting contrast and resolution in the scanning electron microscope. J.Electr.a.Control **7**:97-111.

George EP and Robinson VNE. (1976). The dependence of SEM contrast upon electron penetration, Scanning Electron Microsc. 1976; I:17-26, 738.

George EP and Robinson VNE. (1977a). The influence of electron scattering on the detection of fine topographic detail in the scanning electron microscope (SEM), Scanning Electron Microsc. 1977; I:63-70, 31.

George EP and Robinson VNE. (1977b). Contribution to backscattered electrons discussion. Summary of our views, Scanning Electron Microsc. 1977; I:773-774.

George EP and Robinson VNE. (1980). Fig. 7 **in** Jensen S. and Swyt D. Submicrometer length metrology: Problems, techniques and solutions, Scanning Electron Microsc. 1980; I:400.

Moll SH, Healey F, Sullivan B, and Johnson W. (1978). A high efficiency, nondirectional backscattered electron detector, Scanning Electron Microsc. 1978; I:303-310.

Moll SH, Healey F, Sullivan B, and Johnson W. (1979). Further developments of the converted backscattered electron detector, Scanning Electron Microsc. 1979; II:149-154.

Moncrieff DA and Barker PR. (1978). Secondary electron emission in the scanning electron microscope. Scanning **1**: 195-197.

Peters K-R. (1979). Scanning electron microscopy at macromolecular resolution in low energy mode on biological specimens coated with ultra thin metal films, Scanning Electron Microsc. 1979; II:133-148.

Peters K-R. (1980). Penning sputtering of ultrathin metal films for high resolution electron microscopy, Scanning Electron Microsc. 1980; I:143-154.

Peters K-R. (1982). Validation of George and Robinson SE-I signal theorem. Implication for ultrahigh resolution SEM on bulk untilted specimens. 40th Ann. Proc. Electron Microscopy Soc. Amer., Washington, DC, 1982. G.W. Bailey (ed.), Claitors Publ. Div., Baton Rouge, LA 70821:368-369.

Peters K-R, Schneider BG and Papermaster DS. (1981). Ultrahigh resolution scanning electron microscopy of a periciliary ridge complex of frog retinal rod cells. J. Cell. Biol. **91**:273a.

Reimer L. (1971). Rauschen der Sekundärelektronenemission. Beitr.elektr.mikr.Direktabb.Oberfl. 4/2, Remy Verlag, Münster, W. Germany: 299-304.

Reimer L. (1979). Electron-specimen interaction, Scanning Electron Microsc. 1979; II:111-123.

Reimer L, Seidel H and Gilde H. (1968). Einfluss der Elektronendiffusion auf die Bildentstehung im Raster-Elektronenmikroskop. Beitr.elektr.mikr.Direktabb.Oberfl. **1**:53-56.

Reimer L and Volbert B. (1979). Detector system for backscattered electrons by conversion to secondary electrons. Scanning **2**:238-248.

Seiler H. (1967). Einige aktuelle Probleme der Sekundärelektronenemission. Z.angw.Phys. **22**:249-263.

Swann DJ and Smith KCA. (1973). Lifetime and noise characteristic of tungsten field emitters, Scanning Electron Microsc. 1973:41-48.

Volbert B and Reimer L. (1980). Advantages of two opposite Everhart-Thornley detectors in SEM, Scanning Electron Microsc. 1980; IV:1-10.

Watabe T, Hoshino T and Harada Y. (1976). Observation of individual ferritin particles in the secondary electron mode of scanning electron microscopy. A challenge to immunology using the JEM-100 C/ASID. JEOL News 14e, **1**:11-14.

Wells OC. (1971). Low-loss image for surface scanning electron microscope. Appl. Phys. Lett. **19**:232-235.

Wells OC. (1974). Resolution of the topographic image in the SEM, Scanning Electron Microsc. 1974:1-8, 320, with appendix in Scanning Electron Microsc. 1975:48.

Wells OC. (1975). Measurements of low-loss electron emission from amorphous targets, Scanning Electron Microsc. 1975:43-50, 132.

Wells OC. (1977). Backscattered electron image (BSI) in the scanning electron microscope (SEM), Scanning Electron Microsc. 1977; I:747-771.

Wells OC, Broers AN and Bremer CG. (1973). Methods for examining solid specimens with improved resolution in the scanning electron microscope (SEM). Appl. Phys. Lett. **23**: 353-355.

White EW, McKinstry HA and Johnson GG. (1968). Computer processing of SEM images, Scanning Electron Microsc. 1968; 97-103.